

Triggered Transience of Metastable Poly(phthalaldehyde) for Transient Electronics

Hector Lopez Hernandez, Seung-Kyun Kang, Olivia P. Lee, Suk-Won Hwang, Joshua A. Kaitz, Bora Inci, Chan Woo Park, Sangjin Chung, Nancy R. Sottos, Jeffrey S. Moore,* John A. Rogers,* and Scott R. White*

Transient electronic devices that physically or functionally disintegrate on demand have potential applications, such as biomedical diagnostics, remote environmental sensors, and multifunctional devices with temporal functional profiles. The development of materials with transient properties is critical for the advancement of this technology and its potential application. Hwang et al. demonstrated bioresorbable devices that were successfully fabricated with Mg electrodes, MgO gate dielectrics, Si nano-membrane semiconductor, and silk substrates.^[1] Previous work has focused on demonstrating various classes of transient devices such as high-performance complementary metal-oxide-semiconductor (CMOS) transistors, Si solar cells, strain/temperature sensors, digital-imaging devices, and wireless power-scavenging systems, as well as mechanical energy harvesters and actuators.^[1–5] There is also a variety of metals for electrodes, such as Mo, W, Zn, and Fe; and for encapsulation and passivation materials, such as SiO₂ and SiN_x.^[6,7] Additionally, several biodegradable polymers, such as polycaprolactone, poly(glycolic acid), poly(lactic acid), poly(lactic-co-glycolic acid), have been proposed as suitable substrates for transient electronics.^[8–10]

To the best of our knowledge, previous efforts have focused on achieving transience with devices submerged in a biofluid or aqueous solution. This limits the application of these devices because the life-cycle of the system is solely controlled by the dissolution rate of the materials selected at initial fabrication and the dependence on solution-based degradation largely eliminates non-biological applications. Metastable polymers, such as those with low ceiling temperatures (T_c), and self-immolative polymers, which can be depolymerized rapidly by specific stimuli (triggers), offer a versatile new avenue for materials selection, providing precise control over the lifetime of the transient device and expanding the utility of transient devices beyond dissolution methods alone.^[11–14] We envisage a unique approach towards on-demand physical transience of electronics for a variety of triggering stimuli, such as humidity, temperature, or light. These metastable polymers must fulfill several technical criteria: i) displaying suitable performance as a substrate or encapsulant for microelectronic packaging, ii) undergoing environmentally triggered depolymerization that deactivates the electronics, and iii) allowing for tunable degradation kinetics. Among the metastable polymers reported to date,

H. Lopez Hernandez
Department of Mechanical Science and Engineering
Beckman Institute for Advanced Science and Technology
University of Illinois at Urbana-Champaign
Urbana, IL 61801, USA

Dr. S.-K. Kang
Department of Materials Science and Engineering
Frederick Seitz Materials Research Laboratory
University of Illinois at Urbana-Champaign
Urbana, IL 61801, USA

Dr. O. P. Lee, J. A. Kaitz, Dr. B. Inci, Prof. J. S. Moore
Department of Chemistry, Beckman Institute for
Advanced Science and Technology
University of Illinois at Urbana-Champaign
Urbana, IL 61801, USA
E-mail: jsmoore@illinois.edu

Prof. S.-W. Hwang
KU-KIST Graduate School of Converging Science and Technology
Korea University
Seoul 136-701, Korea

Dr. C. W. Park
Beckman Institute for Advanced Science and Technology
University of Illinois at Urbana-Champaign
Urbana, IL 61801, USA

DOI: 10.1002/adma.201403045

S. Chung
Department of Chemistry, Frederick Seitz Materials
Research Laboratory
University of Illinois at Urbana-Champaign
Urbana, IL 61801, USA

Prof. N. R. Sottos
Department of Materials Science and Engineering
Beckman Institute for Advanced Science and Technology
University of Illinois at Urbana-Champaign
Urbana, IL 61801, USA

Prof. J. A. Rogers
Department of Materials Science and Engineering, Department of
Chemistry, Department of Mechanical Science and Engineering
Department of Electrical and Computer Engineering
Beckman Institute for Advanced Science and Technology
Frederick Seitz Materials Research Laboratory
University of Illinois at Urbana-Champaign
Urbana, IL 61801, USA
E-mail: jrogers@illinois.edu

Prof. S. R. White
Department of Aerospace Engineering, Beckman Institute
for Advanced Science and Technology
University of Illinois at Urbana-Champaign
Urbana, IL 61801, USA
E-mail: swhite@illinois.edu



poly(phthalaldehyde) (PPA) is an ideal candidate for this application due to its low ceiling temperature ($T_c = -43\text{ }^\circ\text{C}$), easy synthesis with various end-groups, and its rapid depolymerization upon backbone bond cleavage.^[15–19] PPA has been used as an acid-degradable photoresist, and its linear, end-functionalized derivatives synthesized by anionic polymerization have been shown to depolymerize selectively in the presence of chemical triggers.^[14,16,20]

Here, we demonstrate photodegradable or phototriggerable transient electronics fabricated on a cyclic PPA (cPPA) substrate with a photo-acid generator (PAG) additive. The electronics are destroyed by triggering the PAG/cPPA substrates with UV light. Transience rates were tuned by modifying the PAG concentration and the irradiance of the UV source. In addition, we demonstrate the encapsulation of a passive device with PAG/PPA. The degradation of the encapsulating film leads to the degradation of the electrode causing an altered performance of the device. We suggest this can be used as a partial triggering technique where only part of a device is destroyed.

cPPA was synthesized by cationic polymerization of *o*-phthalaldehyde (oPA) at $-78\text{ }^\circ\text{C}$ with boron trifluoride diethyl etherate ($\text{BF}_3 \cdot \text{OEt}_2$) as the initiator. Cationic polymerization of oPA produces cyclic polymers with molecular weights that are tuned by changing the initial monomer concentration.^[17] The molecular weights of the cPPA in this study ranged from 114 to 175 kDa (M_n) with PDIs of 2.3 to 2.5. To incorporate UV light sensitivity, we used the PAG 2-(4-methoxystyryl)-4,6-bis(trichloromethyl)-1,3,5-triazine (MBTT), which generates a highly reactive Cl^\cdot radical that abstracts a hydrogen from the environment to form hydrochloric acid (HCl) upon exposure to UV light ($\lambda_{\text{max}} = 379\text{ nm}$).^[21]

cPPA films were solvent-cast onto a polytetrafluoroethylene (PTFE) substrate from solutions in dioxane. Diethylene glycol dibenzoate (DGD) was added as a plasticizer to minimize cracking or breaking of the films during handling. The optimized conditions used a solution of cPPA, MBTT, and plasticizer in dioxane (100 mg cPPA/2.5–5 mg MBTT/2.5 mg DGD/3 mL dioxane). The solution was drop-cast onto PTFE-lined Petri dishes. Subsequent solvent evaporation allowed the removal of free-standing MBTT/cPPA films due to the low adherence

of cPPA to PTFE. The films remain robust under ambient conditions until they are exposed to UV light and begin to rapidly lose their mechanical integrity. The generation of HCl by MBTT leads to the cleavage of the acetal backbone of cPPA, resulting in a rapid depolymerization of the cPPA due to its low T_c . The depolymerization of cPPA films is revealed qualitatively as a transformation from an easily handled free-standing film to an oily and then crystalline residue that agglomerates as time progresses under UV exposure. Our approach to transient electronics using UV triggered cPPA substrates is shown in **Figure 1**. Electronics are fabricated onto MBTT/cPPA films (left) and remain stable until they are exposed to UV light and HCl is generated (middle). After HCl is generated it reacts with the acetal backbone of cPPA and the substrate begins to degrade leading to the destruction of the electronics (right).

IR spectroscopy and dynamic mechanical analysis (DMA) were used to characterize the physical and chemical changes in the MBTT/cPPA films exposed to UV light. IR spectra (**Figure 2a,b**) were taken after MBTT/cPPA was exposed to 365 nm UV light for 180 s. The acetal backbone of cPPA is distinguished by peaks at $900\text{--}1100\text{ cm}^{-1}$. After UV exposure the peak intensity from the acetal backbone decreases while the carbonyl peaks corresponding to reversion to aldehyde monomer at 1700 cm^{-1} appear and grow, indicating a depolymerization reaction to monomer. Two additional peaks not present in the monomer spectrum also emerged at 1766 cm^{-1} and 3383 cm^{-1} (broad) on UV irradiation. We attribute these peaks to the formation of 2-carboxybenzaldehyde, whose IR spectrum displays a peak at 1761 cm^{-1} for the $\text{C}=\text{O}$ stretch and a peak at 3332 cm^{-1} for the acid $-\text{OH}$ stretch.^[22] The presence of 2-carboxyaldehyde is expected because aromatic aldehydes readily oxidize in air.^[15,23]

Given the importance of the mechanical integrity of electronic substrates, the physical degradation of cPPA films was assessed through transient DMA testing. We measured the storage modulus of MBTT/cPPA films while they were continuously exposed to UV to determine the extent and time-scale of degradation. Films containing 2.5% MBTT were tested under two different UV irradiances: 0.70 and 1.75 mW cm^{-2} . The specimens were tested until the UV exposure caused the film

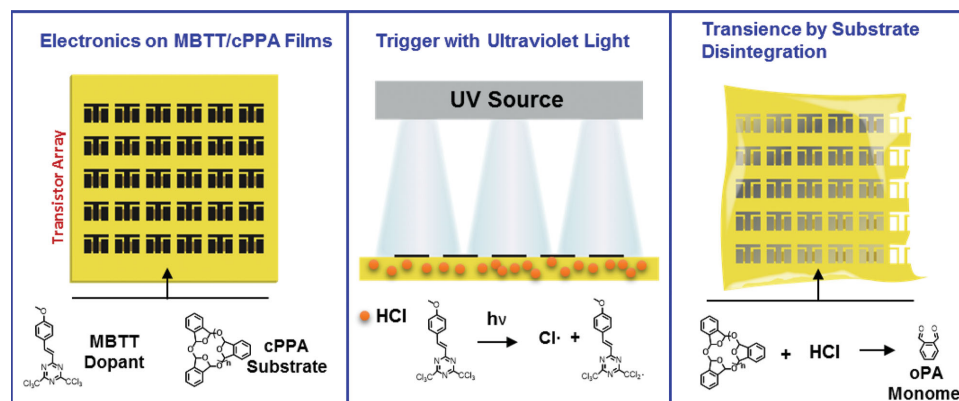


Figure 1. Photoinduced transience of MBTT/cPPA substrate with electronics. Exposing the MBTT/cPPA substrate (left) to UV generates HCl (middle) that causes the rapid depolymerization of the acid sensitive cPPA polymer. This leads to the destruction of the electronics on the substrate (right). In addition to the disintegration of the substrate polymer, generated HCl also degrades the Mg electrodes.

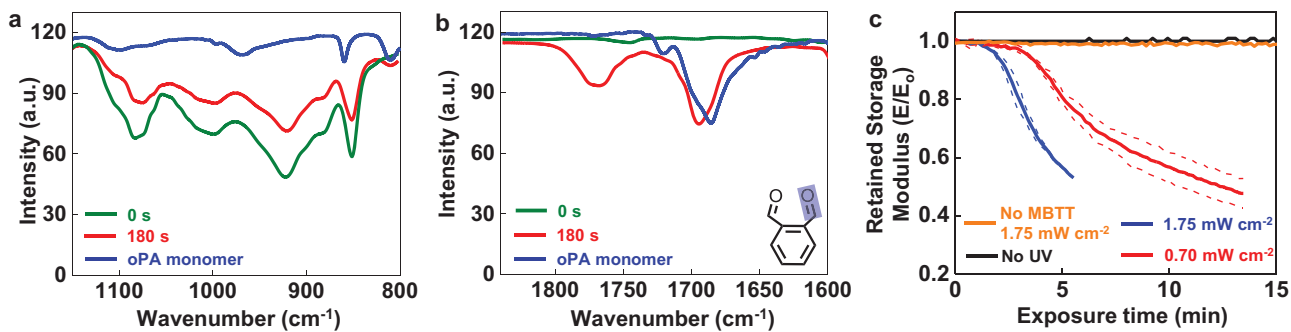


Figure 2. Transient characterization of film properties under UV exposure. FTIR traces of a 2.5% MBTT/cPPA film (5 μm thick) before and after exposure to UV light compared with the oPA monomer. Depolymerization is confirmed by: a) the decrease in intensity of the polymer acetal backbone peaks at 900–1100 cm^{-1} and b) the growth of the monomer carbonyl peak at 1700 cm^{-1} . c) Storage modulus ratio (E_0 = initial storage modulus) of 2.5% MBTT/cPPA films as a function of UV exposure time. The samples were irradiated continuously at the indicated intensity until failure. The solid lines represent the average storage modulus as degradation progresses ($n = 3$). The dashed lines represent one standard deviation from the mean.

to break. The loss in storage modulus during UV exposure is reported in Figure 2c. Significant degradation in storage modulus (up to 66%) is observed prior to failure of the film. The specimens took an average of 7 min to reach failure when exposed to 1.70 mW cm^{-2} and 15 min when exposed to 0.70 mW cm^{-2} . Control samples without any MBTT additive showed a 4% loss of storage modulus when exposed to 1.75 mW cm^{-2} .

Silicon-based active devices were built on the MBTT/cPPA films to demonstrate the feasibility of fabricating functional transient electronic devices. The fabrication of an array of n-channel metal-oxide silicon field-effect transistors (N-MOSFETs) and silicon PIN diodes on MBTT/cPPA substrates was achieved via a combination of a transfer-printing technique and electron-beam (E-beam) deposition (Figure S1, Supporting Information). Since exposing films to UV triggers their degradation, photolithography is incompatible with device fabrication, and avoiding UV exposure of the MBTT/cPPA film during this process is crucial. A silicon nanomembrane (Si NM) (ca. 300 nm thick) was doped and isolated onto a silicon-on-insulator (SOI) wafer (SOITEC, France). It was transfer-printed onto the MBTT/cPPA film with a polydimethylsiloxane (PDMS) stamp after undercutting. The gate oxide (MgO) (ca. 80 nm thick) and metal electrodes (Mg) (ca. 300 nm thick) were deposited by E-beam evaporation through high-resolution stencil masks.

Each N-MOSFET has 30 $\mu\text{m} \times 600 \mu\text{m}$ channel length and width on MBTT/cPPA substrates, and presents typical on/off ratios $> 10^5$ with saturation and linear regime mobilities ca. 350 $\text{cm}^2 \text{V}^{-1} \text{s}^{-1}$ (Figure 3a). Each PIN diode in an array on MBTT/cPPA films consists of a 500 $\mu\text{m} \times 500 \mu\text{m}$ p-doped region, a 500 $\mu\text{m} \times 500 \mu\text{m}$ n-doped region, and a 30 $\mu\text{m} \times 500 \mu\text{m}$ i-region (Figure 3b). The I - V curves show well-defined diode characteristics in which the current is almost negligible under 0.12 V, but begins to increase sharply after 0.49 V. The observed electrical properties are comparable to previously reported devices fabricated in a similar manner on other substrates.^[1,2] Figure 3c shows a free standing 2.5% MBTT/cPPA film with a transistor array exposed to a UV lamp and the physical degradation that occurs over the course of 230 min. The degradation of the substrate leads to the destruction of the onboard electronics.

Triggered degradation of the electronics was demonstrated with serpentine-shaped Mg resistors on MBTT/cPPA substrates (Figure 4a). These devices were placed on a glass slide, attached to a two-probe Wheatstone quarter-bridge setup, and continuously exposed to UV light until the Mg resistors failed. Samples containing 2.5 and 5% MBTT were tested at three different UV irradiances, 0.20, 0.60, and 1.75 mW cm^{-2} . To standardize our analysis of the rate and extent of degradation of devices, we define a resistance increase of 100% as device failure.

After exposure to UV, the cPPA substrates begin to degrade and deform, causing the resistor to degrade and then fail. This deformation is sometimes observed as a sharp increase in resistance, especially for the 2.5% specimens, where the resistance becomes noisy as it approaches failure (Figure 4g). Importantly, once the resistors had failed, the UV-source was removed and the remaining film and Mg traces continued to erode in the presence of the generated acid. Figure 4a–c (2.5% MBTT/cPPA) and Figure 4d–f (5% MBTT/cPPA) show films before testing (left), immediately after failure (middle), and 72 h after failure (right). It can be seen that the Mg traces do not physically disappear after the electronic functionality has been destroyed, but, after 72 h, the sample is almost entirely disintegrated.

We observed that at 1.7 mW cm^{-2} , the MBTT concentration had little effect on the resistance. The resistance of both 2.5 (Figure 4g) and 5% (Figure 4h) samples increased at the same rate and failed within 20 min. At this irradiance, both samples appear to generate sufficient HCl to achieve a maximum degradation rate for the Mg resistor. However, at the lower irradiances of 0.60 and 0.20 mW cm^{-2} , the resistance of the 2.5% specimens degrades more slowly and exhibits a retardation in degradation that does not occur in the 5% samples. The 2.5% samples fail within 90 and 110 min for irradiances of 0.60 and 0.20 mW cm^{-2} respectively, while 5% samples fail within 35 and 70 min. Control samples without any MBTT additive showed a 2.5% increase in resistance at an irradiance of 1.70 mW cm^{-2} .

We also observed that the HCl generated from the MBTT promoted the direct degradation of the Mg electrode.^[24–26] This additional mechanism leads to a coupled packaging–electronic transience in which the MBTT reaction with the Mg and the depolymerization of the cPPA both contribute to degradation of the electronic package. To isolate the role of MBTT on Mg

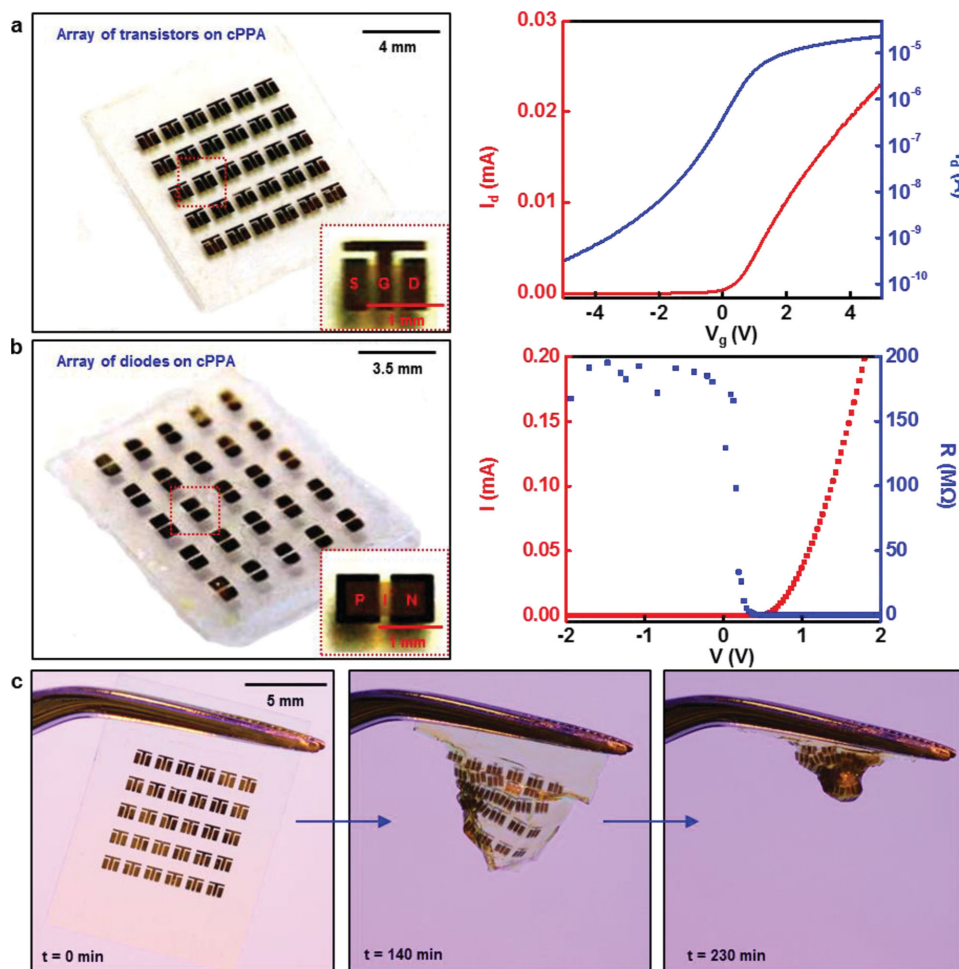


Figure 3. Si active devices on MBTT/cPPA substrates and transience triggered by UV exposure: a) Image (left) and I - V characteristics (right) of N-MOSFET on cPPA with $30 \mu\text{m} \times 600 \mu\text{m}$ channel. The mobility (linear regime) and on/off ratio are ca. $350 \text{ cm}^2 \text{ V}^{-1} \text{ s}^{-1}$ and ca. 10^5 , respectively. b) The array of Si PIN diodes consists of a $500 \mu\text{m} \times 500 \mu\text{m}$ p-doped region, a $500 \mu\text{m} \times 500 \mu\text{m}$ n-doped region, and a $30 \mu\text{m} \times 500 \mu\text{m}$ i-region (left), and its electrical characteristic (right). c) Degradation of a transistor array continuously exposed to 379 nm UV light. The acid generated from UV exposure leads to the destruction of the free-standing transistor array after 230 min.

degradation alone, a Mg resistor was fabricated on a 5% MBTT/polystyrene film and tested under UV exposure (Figure S3 and S4, Supporting Information). The resistance initially increased at the same rate as the 5% MBTT/cPPA sample, but then slowed. The 5% MBTT/polystyrene specimen reached failure after 150 min exposure compared with the 5% MBTT/cPPA, which achieves a similar level of degradation within 20 min.

In addition to the application of MBTT/cPPA films as a transient substrate, we investigated the use of MBTT/cPPA for the encapsulation of Mg resistors. To demonstrate this feature a Mg resistor on a glass substrate was encapsulated with a drop-cast MBTT/cPPA film (Figure 4i) and wired in series with a light-emitting diode (LED). Next, 5 V were applied across the circuit and the encapsulated resistor was exposed to UV (365 nm, 10 mW cm^{-2}). Due to the generation of HCl from the encapsulating film during UV exposure, the Mg protected by the polymer packaging lost conductivity and the LED dimmed as the current in the circuit decreased (Figure 4j). Figure 4k shows the change in resistance for a Mg resistor encapsulated with 2.5%

MBTT/cPPA and exposed to UV light (365 nm, 10 mW cm^{-2}). The concept of selective degradation could enable the modification of future transient devices by partially degrading some portions of their circuits. It is also important to note that this methodology is not limited to Mg electrodes and is open to other acid degradable metal electrodes such as Zn, Fe, and Mo.

The materials system presented here is a toolbox for producing light-triggerable electronics capable of tailorable disintegration of the electronic components. cPPA is a metastable polymer that is readily combined with a PAG to create a photosensitive substrate that has a tunable degradation profile of both its physical properties and the onboard electronic device. We have demonstrated the rapid disintegration of electronics fabricated on an MBTT/cPPA substrate triggered by UV irradiation. The transience time of the electronics was modified by changing the amount of PAG in the polymer films and the UV irradiance. Interestingly, physical transience continues after initial UV light exposure and leads to an unrecognizable residue. This creates a platform for the development

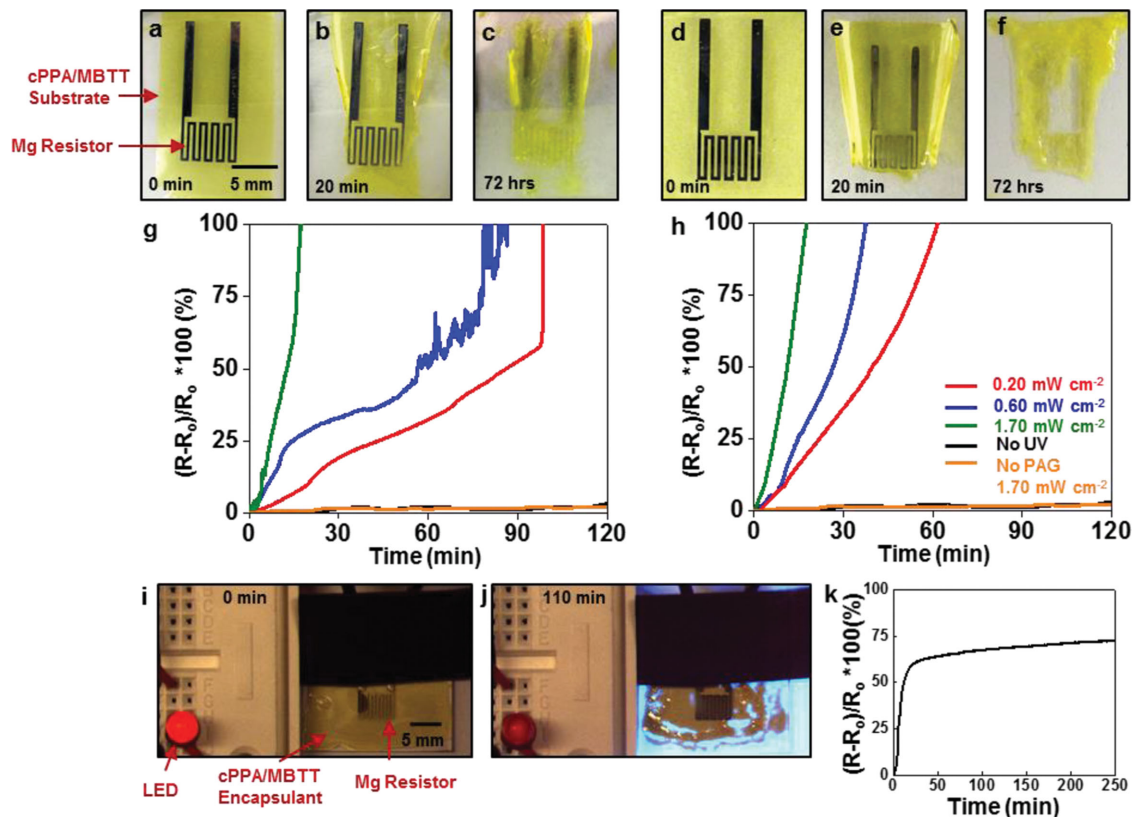


Figure 4. Transient behavior of serpentine Mg resistors. a–f) Physical degradation of a Mg resistor on 2.5% (a–c) and 5% (d–f) MBTT/cPPA substrates before exposure (a,d), after device failure (b,e), and 72 h after testing (c,f). The specimens were continuously exposed to 365 nm UV light and were removed from UV exposure after failure. The image at 72 h demonstrates the continuous degradation that occurs after specimens were triggered by UV light. g,h) The measured resistance of a Mg resistor on a 2.5% (g) and 5% (h) MBTT/cPPA substrate that is continuously exposed to 365 nm UV light. The increase in resistance varies with the irradiance of the UV light source and the concentration of MBTT in the substrate. i,j) Images before (i) and after (j) exposure of a Mg resistor on a glass substrate encapsulated with MBTT/cPPA exposed to 365 nm UV light. The LED is in series with the Mg resistor and dims as the resistor degrades and the resistance increases. k) The resistance data shows the change in resistance of a Mg resistor with a 2.5% MBTT/cPPA encapsulant during UV exposure (365 nm, 10 mW cm⁻²).

of devices that could effectively disappear or dispose of themselves on demand. The partial degradation of an MBTT/cPPA encapsulated Mg resistor suggests the possibility of local selectivity for remapping the current flow of a circuit and changing the functionality of electronics packages. Advances in metastable polymers for transient electronics may lead to more rapid degradation, both physical and electronic, and more varied triggering modalities.

Experimental Section

Fabrication of Transient Electronics (*n*-Channel Silicon MOSFETs, Si PIN Diodes and Mg Resistors): An active region of Si N-MOSFETs and PIN diodes was formed on p-type SOI wafers (SOITECH, France) by phosphorus doping at 950 °C and boron doping at 1000 °C. After the individual device had been isolated by reactive ion etching (RIE), the buried oxide was partially etched by hydrofluoric acid (HF) (49% electronics grade, ScienceLab, USA) to release the silicon nanomembranes (Si NMs). A square-dot (3 μm × 3 μm) square array was patterned and etched by RIE to fully undercut the buried oxide. Si NMs were picked up by PDMS after release from the SOI wafers and transferred to MBTT/cPPA. MgO (ca. 80 nm) was deposited by electron-beam (E-beam) evaporation for the

gate dielectric of the MOSFETs, and Mg (ca. 300 nm) was deposited for the electrodes of the MOSFETs and diodes. A serpentine Mg trace (ca. 300 nm thick) was deposited on the MBTT/cPPA by E-beam evaporation through a stencil mask.

Physical and Chemical Characterization During Transience (Dynamic Mechanical Analysis (DMA) and Fourier-Transform Infrared (FTIR) Spectroscopy): DMA tests were performed at 1 Hz, 0.075% strain amplitude, and a constant static force of 196 mN. cPPA films were cast as described previously and then cut with a punch into rectangular samples of 3.18 mm × 15.88 mm × 40 μm. The gauge length was 10 mm. For FTIR spectroscopy, solutions of 2.5 mg of MBTT/100 mg of cPPA/3 mL of dioxane were made and then cast onto a KBr plate. The film thickness was approximately 5 μm. The film was irradiated at 30-s intervals up to 180 s.

Resistance Measurements of Mg Resistors: The serpentine Mg traces were placed in a Wheatstone quarter-bridge setup, and LabView 2012 was used to monitor the resistance. The resistor was exposed to a UV light (365 nm) at varying distances to tune the irradiance on the sample. The resistance was continuously monitored at 0.5 Hz until the resistance reached a value >1 M Ω.

Supporting Information

Supporting Information is available from the Wiley Online Library or from the author.

Acknowledgements

H.L.H. and S.-K.K. contributed equally to this work. This work was sponsored by the Defense Advanced Research Project Agency with award FA8650-13-C-7347. S.K.K., S.W.H., S.C., and J.A.R. were supported by an NSF INSPIRE grant. The authors thank Dorothy Loudermilk for assistance in figure creation.

Note: The name of author Hector Lopez Hernandez was corrected in the affiliations on December 1, after initial publication online.

Received: July 8, 2014

Revised: August 25, 2014

Published online: October 20, 2014

- [1] S.-W. Hwang, H. Tao, D.-H. Kim, H. Cheng, J.-K. Song, E. Rill, M. A. Brenckle, B. Panilaitis, S. M. Won, Y.-S. Kim, Y. M. Song, K. J. Yu, A. Ameen, R. Li, Y. Su, M. Yang, D. L. Kaplan, M. R. Zakin, M. J. Slepian, Y. Huang, F. G. Omenetto, J. A. Rogers, *Science* **2012**, 337, 1640.
- [2] S.-W. Hwang, D.-H. Kim, H. Tao, T. Kim, S. Kim, K. J. Yu, B. Panilaitis, J.-W. Jeong, J.-K. Song, F. G. Omenetto, J. A. Rogers, *Adv. Funct. Mater.* **2013**, 23, 4087.
- [3] C. Dagdeviren, S.-W. Hwang, Y. Su, S. Kim, H. Cheng, O. Gur, R. Haney, F. G. Omenetto, Y. Huang, J. A. Rogers, *Small* **2013**, 9, 3398.
- [4] S.-W. Hwang, G. Park, H. Cheng, J.-K. Song, S.-K. Kang, L. Yin, J.-H. Kim, F. G. Omenetto, Y. Huang, K.-M. Lee, J. A. Rogers, *Adv. Mater.* **2014**, 26, 1992.
- [5] S.-W. Hwang, X. Huang, J.-H. Seo, J.-K. Song, S. Kim, S. Hage-Ali, H.-J. Chung, H. Tao, F. G. Omenetto, Z. Ma, J. A. Rogers, *Adv. Mater.* **2013**, 25, 3526.
- [6] L. Yin, H. Cheng, S. Mao, R. Haasch, Y. Liu, X. Xie, S.-W. Hwang, H. Jain, S.-K. Kang, Y. Su, R. Li, Y. Huang, J. A. Rogers, *Adv. Funct. Mater.* **2014**, 24, 645.
- [7] S.-K. Kang, S.-W. Hwang, H. Cheng, S. Yu, B. H. Kim, J.-H. Kim, Y. Huang, J. A. Rogers, *Adv. Funct. Mater.* **2014**, 24, 4427.
- [8] H. Acar, S. Çınar, M. Thunga, M. R. Kessler, N. Hashemi, R. Montazami, *Adv. Funct. Mater.* **2014**, 24, 4135.
- [9] S.-W. Hwang, J.-K. Song, X. Huang, H. Cheng, S.-K. Kang, B. H. Kim, J.-H. Kim, S. Yu, Y. Huang, J. A. Rogers, *Adv. Mater.* **2014**, 2, 3905.
- [10] S.-W. Hwang, G. Park, C. Edwards, E. A. Corbin, S.-K. Kang, H. Cheng, J.-K. Song, J.-H. Kim, S. Yu, J. Ng, J. E. Lee, J. Kim, C. Yee, B. Bhaduri, Y. Su, F. G. Omenetto, Y. Huang, R. Bashir, L. Goddard, G. Popescu, K.-M. Lee, J. A. Rogers, *ACS Nano* **2014**, 8, 5843.
- [11] S. Köstler, *Polym. Int.* **2012**, 61, 1221.
- [12] A. Esser-Kahn, N. Sottos, S. R. White, J. S. Moore, *J. Am. Chem. Soc.* **2010**, 132, 10266.
- [13] O. Coulembier, A. Knoll, D. Pires, B. Gotsmann, U. Duerig, J. Frommer, R. D. Miller, P. Dubois, J. L. Hedrick, *Macromolecules* **2010**, 43, 572.
- [14] W. Seo, S. T. Phillips, *J. Am. Chem. Soc.* **2010**, 132, 9234.
- [15] A. M. DiLauro, J. S. Robbins, S. T. Phillips, *Macromolecules* **2013**, 46, 2963.
- [16] M. Tsuda, M. Hata, *J. Polym. Sci., Part A: Polym. Chem.* **1997**, 35, 77.
- [17] J. A. Kaitz, C. E. Diesendruck, J. S. Moore, *J. Am. Chem. Soc.* **2013**, 135, 12755.
- [18] C. E. Diesendruck, G. I. Peterson, H. J. Kulik, J. A. Kaitz, B. D. Mar, P. A. May, S. R. White, T. J. Martínez, A. J. Boydston, J. S. Moore, *Nat. Chem.* **2014**, 6, 623.
- [19] A. W. Knoll, D. Pires, O. Coulembier, P. Dubois, J. L. Hedrick, J. Frommer, U. Duerig, *Adv. Mater.* **2010**, 22, 3361.
- [20] A. M. DiLauro, A. Abbaspourrad, D. A. Weitz, S. T. Phillips, *Macromolecules* **2013**, 46, 3309.
- [21] G. Pohlers, J. Scaiano, R. Sinta, R. Brainard, D. Pai, *Chem. Mater.* **1997**, 9, 1353.
- [22] IR spectrum of 2-carboxybenzaldehyde (CAS# 119-67-5) in Spectral Database for Organic Compounds (SDBS), http://sdfs.db.aist.go.jp/sdfs/cgi-bin/direct_frame_disp.cgi?sdfsno=1691, accessed: September **2014**.
- [23] S. P. Tucker, *J. Environ. Monit.* **2008**, 10, 1337.
- [24] B. Roald, W. Beck, *J. Electrochem. Soc.* **1951**, 98, 277.
- [25] M. Kilpatrick Jr., J. Rushton, *J. Phys. Chem.* **1930**, 34, 2180.
- [26] M. Kilpatrick Jr., J. Rushton, *J. Phys. Chem.* **1934**, 38, 269.